



Enhancement in energy and exergy efficiency of a solar receiver using suspended alumina nanoparticles (nanofluid) as heat transfer fluid

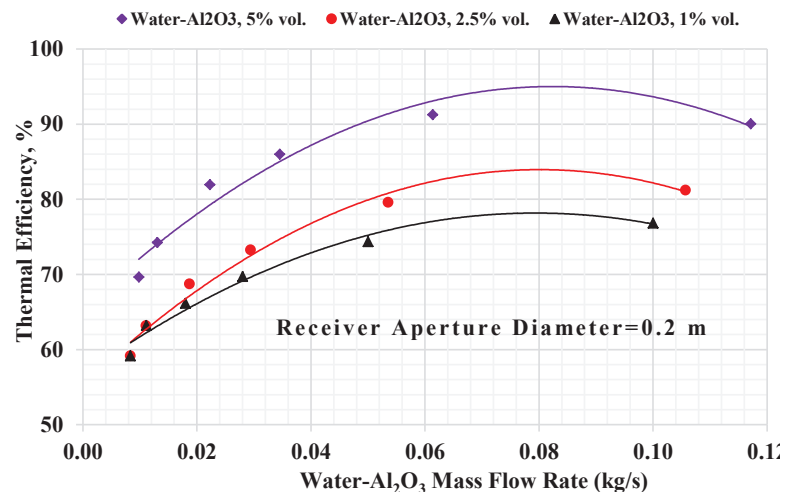
Vahid Madadi, Amir Rahimi, Touraj Tavakoli*

*Department of Chemical Engineering, Faculty of Engineering, University of Isfahan, 81746-73441, Isfahan, Iran

HIGHLIGHTS

- An experimental and theoretical energy and exergy analysis performed for a solar receiver.
- A simplified Nusselt number for heat transfer fluid through the receiver was proposed.
- Suspended alumina nanoparticles (nanofluids) were used as heat transfer fluids.
- The effect of suspended alumina nanoparticles on efficiency of solar receiver was studied.
- The effect of nanoparticle volume fraction on exergy efficiency was investigated.

GRAPHICAL ABSTRACT



ARTICLE INFO

Article history:

Received 13 December 2014
Received in revised form
29 December 2014
Accepted 5 January 2015

Keywords:

Exergy efficiency
Thermal efficiency
Receiver
Alumina nanoparticles
Nanofluid

ABSTRACT

An experimental and theoretical energy and exergy analysis was conducted for a cylindrical cavity receiver employed in a parabolic dish collector. Based on simultaneous energy and exergy analysis, the receiver average wall temperature and overall heat transfer coefficient were determined. A simplified Nusselt number for heat transfer fluid (HTF) through the receiver as a function of Reynolds and Prandtl numbers was proposed. Based on correlated Nusselt number, the effects of two nanofluids of alumina nanoparticles in water and ethylene glycol as base fluid on the performance of system were investigated. When nanofluids are employed as HTF through the receiver, the energy and exergy efficiency are greater compare to pure water. The minimum enhancement in receiver thermal efficiency is 25% and enhancement greater than 60% is attainable. The results indicate that, by increasing only 5% volume in nanoparticle concentration in water, the receiver thermal efficiency is increased greater than 20%. The effect of nanoparticles volume fraction on exergy efficiency for small HTF mass flow rates is greater than larger mass flow rates. By selecting only 5% volume of alumina nanoparticle in water, for small HTF mass flow rates, enhancement in exergy efficiency greater than 10% is attainable.

1. Introduction

Global utilization of fossil fuels leads to a significant increasing in greenhouse gas emissions and pollutants and this important issue stimulated researchers to pursue and promote research related to renewable energy sources, especially solar energy. Among the renewable energies, solar energy is very popular because of being rich, free, pollution free and available. Solar energy is widely used in most industries and building applications. However, the application of solar energy has not yet been developed enough. During the last two decades, the worldwide research in the field of solar energy has focused on the methods to efficiency enhancement of the solar collection and conversion systems. Solar concentrator collectors in comparison with the other type of solar collector, such as: flat plate collectors and parabolic through collectors, are more efficient and capable technologies for achieving high temperatures. The high temperature heat production from solar energy can be accomplished by a concentrator and a focal absorber or receiver. The solar parabolic dish collector also has more advantages over others of its kind due to its low heat loss features, high geometric concentration ratio and creation of high temperature [1]. Therefore, some imperfections such as defective mechanical structure of the system and high thermal resistance of HTF through the receiver can reduced the performance of the system. For existing solar collectors, one of the most effective methods for enhancing thermal efficiency of the systems, is replacing their heat transfer fluid with high thermal conductivity fluids. Nanofluids are suspensions of nano-sized particles in a base fluid. A substantial increase in liquid thermal conductivity, liquid viscosity and heat transfer coefficient. Nanofluids are expected to present exceptional heat transfer properties compared with conventional heat transfer fluids. Before now, many studies have been conducted about using nanofluids in solar collectors. The environmental and economic impacts of using nanofluids to enhance solar collector efficiency as compared to conventional solar collectors for domestic hot water systems were investigated by Otanicar *et al.* [2]. Yousefi *et al.* have investigated the effect of Al_2O_3 - H_2O nanofluid on the efficiency of a flat plate solar collector. In this study, authors showed that using this nanofluid, with 0.2 wt% of nanoparticles, as working fluid increases the collector efficiency about 28.3% [3]. Lu *et al.* have used deionized water and water-based CuO nanofluids as the working fluid in an evacuated tubular solar collector and the thermal performance of the system have been studied. Their

experiment results showed that by using CuO nanofluid, a significant enhancement in thermal performance of the system can be achieved and the evaporating heat transfer coefficient may increase by about 30% compared with those of deionized water [4]. The effects of three different nanofluids, Al_2O_3 , ZnO and MgO in water as the base fluid, on the performance of a tubular solar collector have been investigated by Li *et al.* [5]. Authors concluded that ZnO- H_2O nanofluid with 0.2% volume concentration is the best selection for the collector. Khullar *et al.* investigated theoretically thermal performance of a nanofluid-based concentrating parabolic solar collector (NCPSC). The Aluminum nanoparticles with 0.05% in volume suspended in Therminol as the base fluid was used in the mentioned work. The authors compared the results with the experimental results of conventional concentrating parabolic solar collectors operating under similar conditions and the results revealed that the thermal efficiency of NCPSC is increased about 5-10% [6]. Taylor *et al.* studied the effect of nanofluids made from graphite nanoparticles on the performance of high flux solar collectors and showed that using the nanofluids enhances the efficiency up to 10% [7].

One of the most important aspects of thermal analysis of solar collectors is heat losses analyses. In parabolic solar dish collectors, (PSDC) the heat is lost from the receiver (which is the most important component of the system) to the ambient by convection, conduction and radiation mechanisms. The amount of conduction heat losses compare with two other mechanisms is negligible. The heat losses from the receiver to the ambient has significant effect on performance of the system. Many experimental and numerical investigations have been carried out on the natural convection heat transfer in cavity receivers with different configurations, like: square, rectangular, cylindrical, and spherical. An analytical model was presented for estimation of convective heat loss from a cubical cavity receiver based on the local heat transfer coefficient inside the receiver, and heat and mass transferred by the air through the aperture due to buoyancy and wind effects [8]. The thermal performance of cavity receivers of a low-cost solar parabolic dish are characterized and optimized by Kaushika and Reddy [9]. Three types of receivers were studied comprehensively for a fuzzy focal solar dish concentrator by Sendhil and Reddy [10]. Two different types of receivers, semi-cavity and modified cavity are proposed by Kaushika where both receivers have higher efficiency than others of this kind [11].

Authors in [12] studied the thermal performance of a multistage solar receiver and minimized the heat losses by dividing the aperture into two stages according to the irradiance distribution levels. The heat transfer aspects of the high temperature receiver and the losses due to partitioning the receiver are discussed in this study. A high temperature cavity receiver for residential scale application was designed by Matthew and Hohyun. [13]. Wang et al. conducted a numerical simulation of the heat flux distribution in a solar cavity receiver [14]. The radiative heat transfer in a closed cavity solar receiver for high temperature solar thermal processes was evaluated by finite volume solutions [15]. Prakash et al. determined the stagnation and convective zones in a solar cavity receiver. In this study, the experimental and numerical studies were carried out to identify these zones [16].

In thermal analysis of solar cavity receivers, two main approaches exist. In the first, it is assumed that the all component of the receiver inner surface have a constant temperature and the inner surface of the solar receiver is isothermal and in the second approach, constant solar radiation flux is considered and it is assumed that a constant heat flux incident to the inner surface of the receiver. In this study, the first approach is applied. In thermal analysis with isothermal receiver wall condition, two important issues must be determined. The receiver average wall temperature and overall heat transfer coefficient. By good insulating of receiver external surface, the conductive heat loss is negligible and radiative and convective heat losses from the inner surface of the receiver to the ambient is dominant. In the most previous thermal analyses of solar receivers, the researchers conducted that the radiative heat losses from the receiver can be determine analytically. But, since the various system operational and structural parameters have significant effects on the convective heat loss, the convective heat analysis, especially in present of the wind, is more complicated. On the other hand, experimentally determining the average receiver wall temperature is difficult and in some cases is impossible. According to the mentioned explanations, by applying only the energy analysis of the system (first thermodynamic law analysis), thermal analysis of the system to define the system performance is weak and cannot be trusted.

In the present work, a constructed solar parabolic dish with a cylindrical cavity receiver is studied. Based on new technique, the first and second thermodynamic law analyses (simultaneous energy and exergy analyses) are applied to thermal analysis of the system.

From energy and exergy analysis the average receiver wall temperature and overall heat transfer coefficient are determined. In our previous work, an energy and exergy analysis was carried out for the system under study [17]. By an energy balance on the heat transfer fluid (HTF) through the receiver, a simplified and applicable correlation for the Nusselt number to estimate the amount heat transfer from the receiver surface to the HTF is provided. A correlation for Nusselt number as a function of HTF Reynolds number and Prandtl number is proposed. Based on proposed Nusselt number, the effects of thermal properties of some nanofluid as HTF through the receiver on the energy and exergy efficiency of the system are investigated.

2. Experiments and methods

The system under study consists of a parabolic dish concentrator with a cylindrical receiver which is employed in the center of dish. Two supporting adjustable metal arms are installed on the dish frame to adjust the receiver on the focal center of the dish. A photo of dish with cylindrical receiver is shown in Fig. 1. The dish aperture diameter and focal length are 2.88 and 1.5 m respectively. The sunlight tracking is manual. Three receiver aperture diameters, 0.115, 0.14 and 0.2 m were applied in experiments. The receiver height is 0.4 m and HTF moves in a spiral path with 0.03 m gap space. The mirrors are stuck on the metal surface and the entire system is installed on a concrete foundation.

Through experiments, two parameters of HTF is measured, HTF temperature and mass flow rate. The HTF inlet and outlet temperatures are measured by two PT100 RTD thermocouples, and the temperatures are shown in a digital monitor which is installed in the back of the dish. The HTF inlet temperature range was 285 to 325 K. Also, a flow meter is used to measure the HTF mass flow rate and a range between 0.007 up to 0.5 kg/s were tested. The ambient air temperature and velocity are measured by Lutron ANEMOMETER/HUMIDITY METER Model AM-4205A device. The amount of solar irradiance is measured by two devices for more accuracy, TES-1333/ TES-1333R Solar Power Meter and TES-132 Solar Power Meter.

3. Energy and exergy analysis

For short period of time it is reasonable to assume that the system is in steady state condition due to small changes in solar irradiance.

For steady state conditions, the energy balance for the cylindrical receiver (control volume shown in Fig. 1) can be written as following equation:

$$\eta_o I_b A_c + \dot{m} c_p (T_{in} - T_{out}) - \dot{Q}_{l,conv.} - \dot{Q}_{l,rad.} = 0 \quad (1)$$

where, η_o is the optical efficiency which is defined as the amount of reflected solar irradiance from the concentrator to the receiver and in this study is calculated about 0.75. In Eq. (1), I_b is global solar irradiance, A_c is concentrator aperture area, $\dot{Q}_{l,conv.}$ and $\dot{Q}_{l,rad.}$ are the rates of heat which are lost by convection and radiation mechanisms respectively.

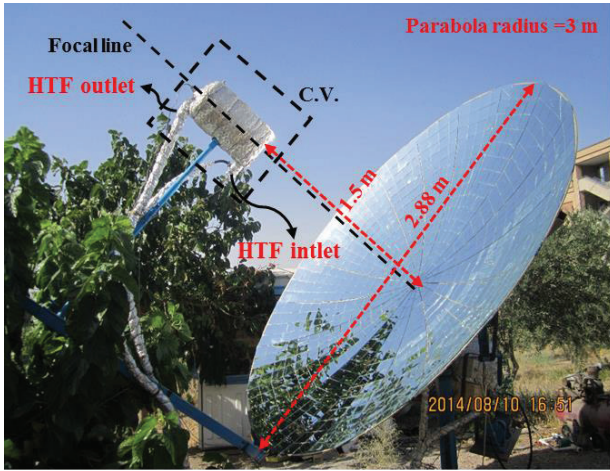


Fig. 1. The photo of dish with cylindrical receiver.

The rate of radiation heat loss can be estimated from the following equation [18]:

$$\dot{Q}_{l,rad.} = \varepsilon_{eff} \sigma A_{r,ap} (T_w^4 - T_a^4) \quad (2)$$

where, σ is Stefan–Boltzmann constant, $A_{r,ap}$ is receiver aperture area, T_w and T_a are average receiver wall and ambient temperatures respectively. The ε_{eff} is effective emissivity and is based on the receiver total surface area and is given by [19]:

$$\varepsilon_{eff} = \frac{1}{1 + \left(\frac{1 - \varepsilon}{\varepsilon} \right) \frac{A_{r,ap}}{A_{r,w}}} \quad (3)$$

By combining Eqs. (1) and (2), the energy balance for receiver can be rewritten as below:

$$\eta_o I_b A_c + \dot{m} c_p (T_{in} - T_{out}) - U_l A_{r,ap} (T_w - T_a) - \varepsilon_{eff} \sigma A_{r,ap} (T_w^4 - T_a^4) = 0 \quad (4)$$

In Eq. (4), two unknown parameters must be found to thermal analysis of the system and determine the system performance. The receiver average wall temperature, T_w and convection overall heat transfer coefficient, U_l . So, we need another equation. By applying the second thermodynamic law at steady state condition for selected C.V. shown in Fig. 1, the two unknown parameters can be defined. The exergy balance for the C.V. is given by:

$$\sum \dot{E}_{in} - \sum \dot{E}_{out} - \sum \dot{E}_{loss} - \sum \dot{E}_{des} = \sum \dot{E}_{change} \quad (5)$$

At steady state condition, the amount of exergy changes in the system is zero. In such systems, the input exergy rate includes the exergy flow rate coming from the HTF and exergy rate of solar irradiance which is reflected from concentrator to the receiver. For the control volume shown in Fig. 1, the total rate of exergy input is:

$$\sum \dot{E}_{in} = \left[\dot{m} c_p \left(T_{in} - T_0 - T_0 \ln \frac{T_{in}}{T_0} \right) + \frac{\dot{m} \Delta P_{in}}{\rho} \right] + \psi \eta_o I_b A_c \quad (6)$$

where, T_0 is dead state temperature, ΔP_{in} is pressure difference between inlet HTF to the receiver and ambient pressure and ψ is maximum useful work available from radiation.

Until now, many studies have been conducted to investigate the amount of work available from radiation reservoirs [20-24]. The Petela-Landsberg efficiency corresponds to the fully concentrated radiation. However, the system under study in this paper is not a fully concentrator. Therefore, the Petela-Landsberg formula is not appropriate. The appropriate equation to calculate the amount of ψ in this study, is given by [22]:

$$\psi = 1 - \frac{4T_0}{3T_s} + \frac{1}{3f_H} \left(\frac{T_0}{T_s} \right)^4 \quad (7)$$

where, T_s is black body sun temperature and is considered about 5800 K [25], and the f_H is the geometric factor and is given by Eq. [22]:

$$f_H = \frac{\Omega}{\pi} \left(1 - \frac{\Omega}{4\pi} \right) \cos(\theta_0) \quad (8)$$

In Eq. (8), Ω is the solid angle subtended by the mirrors and θ_0 is the zenith angle. The solid angle is given by [22]:

$$\Omega = 2\pi(1 - \cos \delta) \tag{9}$$

where, δ is the half-angle of the cone subtending the concentrator when viewed from the receiver. For the system under study, the geometric factor was calculated about 0.6.

The exergy output rate only include the exergy outflow rate from the HTF existing the solar receiver and is calculated from the Eq. (10)

$$\sum \dot{E}_{out} = \dot{m}c_p \left(T_{out} - T_0 - T_0 \ln \frac{T_{out}}{T_0} \right) + \frac{\dot{m} \Delta P_{out}}{\rho} \tag{10}$$

For the control volume shown in Fig. 1, the rate of exergy losses is due to heat transfer losses from the solar receiver to the ambient. Therefore, the total rate of exergy losses is given by [26]:

$$\sum \dot{E}_{loss} = \dot{Q}_{loss} \left(1 - \frac{T_0}{T_w} \right) \tag{11}$$

In the solar receivers, the exergy destruction is caused by HTF pressure drop through the receiver and heat transfer from high to low temperatures [26]. The rate of exergy destruction due to HTF pressure drop is as follows [27]:

$$\dot{E}_{des, \Delta p} = T_0 \frac{\dot{m} \Delta p}{\rho} \frac{\ln(T_{out}/T_{in})}{T_{out} - T_{in}} \tag{12}$$

In such systems, the exergy destruction due to heat transfer from high to low temperatures includes exergy destruction due to solar energy absorption by receiver and exergy destruction due to heat conduction from the receiver wall to the HTF. Therefore, the total rate of the exergy destruction due to heat transfer is given by [26, 28]:

$$\dot{E}_{des, heat} = \dot{m}c_p (T_{out} - T_{in}) T_0 \left(\frac{1}{T_w} - \frac{1}{T_s} \right) + \dot{m}c_p T_0 \left(\ln \frac{T_{out}}{T_{in}} - \frac{T_{out} - T_{in}}{T_w} \right) \tag{13}$$

where, the first term in right hand side of Eq. (13) is the rate of exergy destruction due to solar energy absorption and the second term is the rate of exergy destruction due to heat conduction from the receiver wall to the HTF.

By combining Eqs. (6) -(13) and general exergy balance equation, Eq. (5), the exergy balance equation can be rewritten as follows:

$$\psi \eta_o I_b A_c - \dot{m}c_p (T_{out} - T_{in}) \left(1 - \frac{T_0}{T_s} \right) - \dot{Q}_l \left(1 - \frac{T_0}{T_w} \right) - \frac{\dot{m} \Delta p}{\rho} \left(1 - \frac{T_0}{T_{lm}} \right) = 0 \tag{14}$$

where, T_{lm} is HTF log-mean temperature difference at inlet and outlet. By combining the energy balance equation, Eq. (4), and exergy balance equation, Eq. (14), two unknown parameters; average receiver wall temperature, T_w , and overall convective heat transfer coefficient, U_p can be obtained.

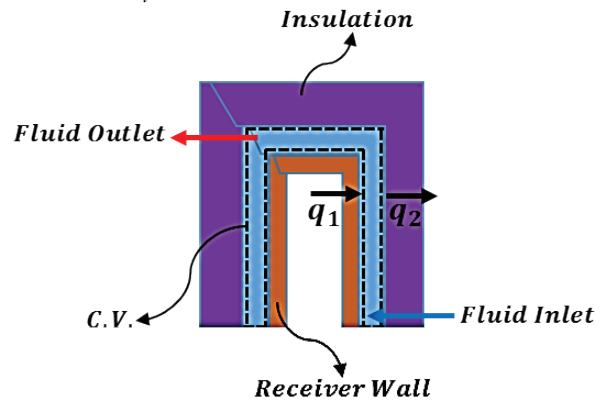


Fig. 2. schematic control volume for the HTF flowing through the receiver.

The schematic control volume for HTF through the receiver is shown in Fig. 3. The HTF temperature through the receiver is increased due to convection heat transfer from the inner surface of the receiver to the HTF. Conductive heat losses from the receiver external surface to the ambient can be assumed negligible due to good insulation. The internal convection heat transfer coefficient through the receiver can be found by an energy balance around the inner surface of the receiver as follows:

$$hA (T_w - T_b) = \dot{m}c_p (T_{out} - T_{in}) \tag{15}$$

where, T_b is the HTF bulk temperature and can be considered as log mean temperature difference at outlet and inlet HTF temperatures, e.g. T_{lm} .

The heat transfer from the receiver surface to the HTF is forced convection and based on general form

of Nusselt number as a function of Reynolds and Prandtl numbers can be given by:

$$Nu_d = \frac{hd}{k} = c Re^n Pr^m \quad (16)$$

where, d is characteristic length of receiver, k is HTF thermal conductivity, c , n and m are constants. By combining Eqs. (15) and (16), the Nusselt number is calculated by experimental data fitting as follows:

$$Nu_d = \frac{\dot{m}c_p (T_{out} - T_{in}) d}{A (T_w - T_{lm}) k} = c Re^n Pr^m \quad (17)$$

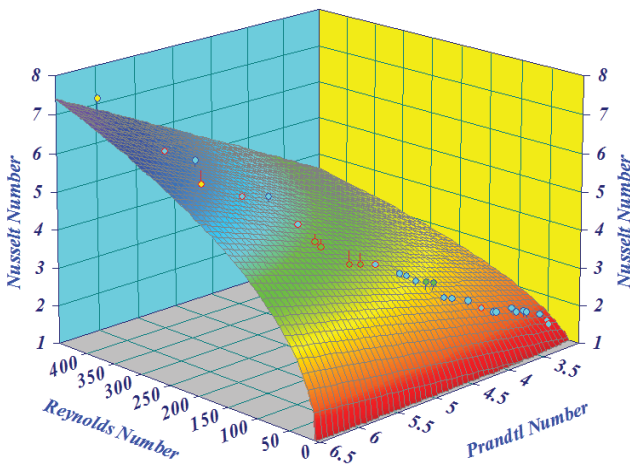


Fig. 3. A 3D plot of Nusselt number as a function of Reynolds and Prandtl numbers.

A 3D plot of Nusselt number as a function of Reynolds and Prandtl numbers is shown in Fig. 2. The correlated Nusselt number from experimental data fitting is given as:

$$Nu_d = 0.12514 Re^{0.38001428} Pr^{0.94011676} \quad 30 < Re < 500 \quad (18)$$

For Eq. (18), the R^2 is greater than 0.98. The Eq. (18) is an applicable equation, because can be used in thermal analysis of solar cylindrical cavity receivers for various HTFs flowing through the receiver such as nanofluids.

The exergy balance for the C.V. shown in Fig. 3 is written as:

$$\left(1 - \frac{T_0}{T_{lm}}\right) \dot{Q}_1 - \left(1 - \frac{T_0}{T_{lm}}\right) \dot{Q}_2 + \dot{m} [(h_{in} - h_{out}) - T_0 (s_{in} - s_{out})] - \dot{E}_{d,\Delta P} = 0 \quad (19)$$

The destructed exergy due to HTF pressure drop and conductive heat loss is negligible. Therefore, the Eq. (19) is simplified as:

$$\left(1 - \frac{T_0}{T_{lm}}\right) \dot{Q}_1 + \dot{m} c_p \left[(T_{in} - T_{out}) - T_0 \ln \frac{T_{in}}{T_{out}} \right] = 0 \quad (20)$$

Since the internal convection coefficient through the receiver is calculated from the correlated Nu number, for various HTF through the receiver such as nanofluids with known inlet temperature and mass flow rate, the thermal analysis of such system can be done. Two unknown parameters, HTF outlet temperature and receiver average wall temperature is calculated by simultaneous energy and exergy analysis, by applying Eqs. (15) and (20).

The receiver thermal efficiency is defined as the ratio of the heat delivered by HTF through the receiver to the amount of solar energy reflected from concentrator. Therefore, the receiver thermal efficiency is calculate from the following equation:

$$\eta_{th,r} = \frac{\dot{m}c_p (T_{out} - T_{in})}{\eta_o A_c I_b} \quad (21)$$

The receiver exergy efficiency is defined as the ratio of the gained exergy by HTF to the total exergy input from concentrator and is given by;

$$\eta_{ex,r} = \frac{\dot{m}c_p \left(T_{out} - T_{in} - T_0 \ln \frac{T_{out}}{T_{in}} \right) - \frac{\dot{m} \Delta P_{HTF}}{\rho}}{\psi \eta_o A_c I_b} \quad (22)$$

4. Research methodology

The aim of this work is to propose a simplified Nusselt number for HTF through the receiver. The HTF for the system under study is water. By an energy and exergy balance (Eqs. (1) and (14)) for the system shown in Fig. 1, the receiver average wall temperature and overall heat transfer coefficient for heat transfer from the receiver inner surface to the ambient are determined. Based on energy balance on the receiver inner surface and HTF through the receiver, Eq. (15), convection heat transfer through the receiver is estimated. By using the Eq. (16) and obtained experimental data, a Nusselt number correlation for HTF through the receiver as a function of Reynolds and Prandtl numbers

numbers is proposed. All properties are calculated at mean temperature. By applying correlated Nusselt number, energy and exergy balance for HTF through the receiver, Eqs. (18), (15) and (20) respectively, for various HTF with known parameters such as inlet temperature, outlet temperature and mass flow rate, the HTF unknown parameter and receiver average wall temperature are calculated and thermal performance of the receiver with various nanofluids as HTF through the receiver is studied.

5. Results and discussion

In this study, to investigate thermal performance of the solar receiver with nanofluids as HTF, alumina nanoparticles in two base fluids, water and ethylene glycol (EG) are considered. Three volume fractions of nanoparticle in base fluid are selected to investigate the effect of nanoparticle volume fraction on energy and exergy efficiency of receiver. According to literature survey [29], the density of nanofluids is calculated by following equation:

$$\rho_{nf} = \phi\rho_{np} + (1 - \phi)\rho_{bf} \quad (23)$$

where, ρ_{nf} , ρ_{np} and ρ_{bf} are nanofluid, nanoparticle and base fluid density respectively. In Eq. (23) ϕ is the volume fraction of nanoparticles in base fluid. The specific heat capacity of nanofluids is calculated from Eq. (24) [29-31].

$$c_{p,nf} = \frac{\phi\rho_{np}c_{p,np} + (1 - \phi)\rho_{bf}c_{p,bf}}{\rho_{nf}} \quad (24)$$

The temperature dependency of nanofluid thermal conductivity and dynamic viscosity for Water- Al_2O_3 and EG- Al_2O_3 with 1, 2.5 and 5% volume fraction is shown in Table 1 [32].

Table 1.
Dynamic viscosity and thermal conductivity of samples as a function of T(°C)

Samples	Thermal Conductivity(W/m.K), T(°C)	Dynamic Viscosity(cP), T(°C)
1% Al_2O_3 -EG	$k_{nf} = 0.2244exp^{0.0057T}$	$\mu_{nf} = 50.131exp^{-0.039T}$
2.5% Al_2O_3 -EG	$k_{nf} = 5.79 \times 10^{-5}T^2 - 3.06 \times 10^{-3}T + 0.2993$	$\mu_{nf} = 48.066exp^{-0.025T}$
5% Al_2O_3 -EG	$k_{nf} = 1.00 \times 10^{-4}T^2 - 7.50 \times 10^{-3}T + 0.4411$	$\mu_{nf} = 566.66exp^{-0.866T}$
1% Al_2O_3 - H_2O	$k_{nf} = 6.37 \times 10^{-4}T^2 - 0.0304T + 1.0552$	$\mu_{nf} = 10.056exp^{-0.637T}$
2.5% Al_2O_3 - H_2O	$k_{nf} = 3.87 \times 10^{-4}T^2 - 1.3 \times 10^{-2}T + 0.7173$	$\mu_{nf} = 32.104exp^{-0.856T}$
5% Al_2O_3 - H_2O	$k_{nf} = 7.43 \times 10^{-4}T^2 - 0.0463T + 1.3514$	$\mu_{nf} = 22046exp^{-2.255T}$

5.1. Effect of HTF mass flow rate on receiver thermal efficiency

The effect of HTF mass flow rate through the receiver on receiver thermal efficiency for three fluids, water, water- Al_2O_3 and EG- Al_2O_3 for receiver aperture diameter (RAD) equal to 0.115 is shown in Fig 4. By an increasing in HTF mass flow rates, the receiver thermal efficiency is increased until the thermal efficiency is reached to its maximum value at a specific value of mass flow rate and then decreases due to reduction in temperature difference. Results in Fig. 4 indicated that, when the alumina nanoparticles in water and ethylene glycol compare to water is employed as HTF through the receiver, the thermal efficiency is greater. The minimum enhancement in receiver thermal efficiency is 25% and enhancement greater than 60% is attainable when nanofluids are employed as HTF through the receiver.

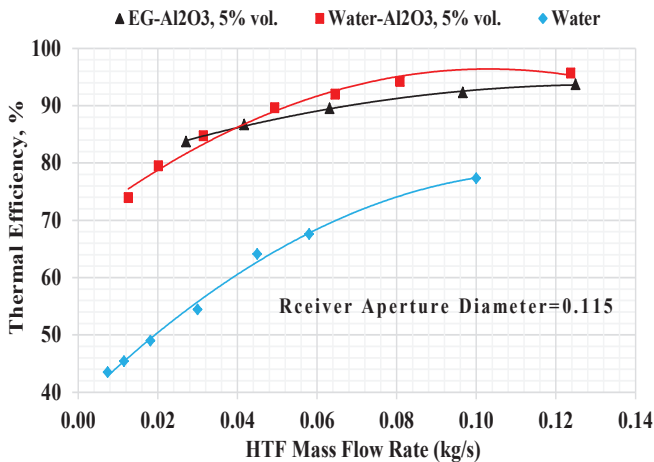


Fig. 4. Effect of HTF mass flow rate on receiver thermal efficiency.

5.2. Effect of nanoparticle volume fraction on receiver thermal efficiency

The effect of water- Al_2O_3 mass flow rate on receiver thermal efficiency for three volume fraction of alumina nanoparticles is shown in Fig. 5. Results show that, for nanofluid with greater nanoparticle volume fraction, the receiver thermal efficiency is greater. It can be explained that for greater nanoparticle volume fractions, the nanofluid thermal conductivity is greater and consequently the thermal efficiency is greater due to greater heat transfer through the receiver.

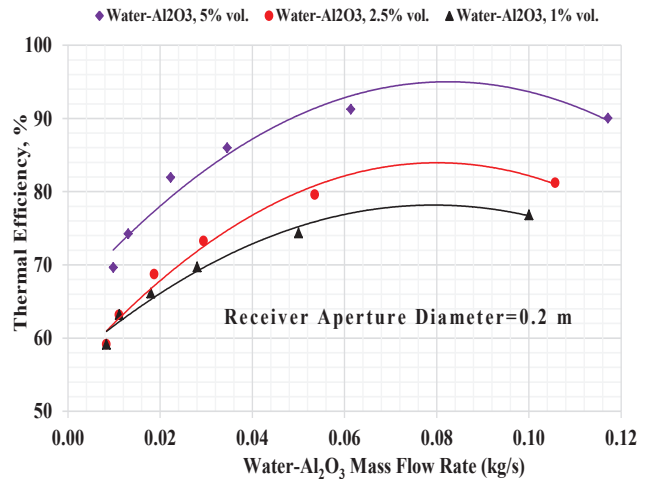


Fig. 5. Effect of alumina nanoparticle volume fraction on receiver thermal efficiency.

By an increasing in nanoparticle concentration in base fluid, the nanofluid viscosity is increased significantly, and consequently, the pressure drop through the receiver is increased but, the effect of pressure drop through the receiver can be explained by energy analysis of the system (first thermodynamic law analysis) and when the pressure drop is high, the system exergy analysis (second thermodynamic law analysis) must be carried out. The results in Figs. 4 and 5 also revealed that, by increasing only 5% volume in nanoparticle concentration in water, the receiver thermal efficiency is increased greater than 20% compare to pure water.

5.3. Effect of HTF mass flow rate on receiver exergy efficiency

The effect of HTF mass flow rate on receiver exergy efficiency is shown in Fig. 6. By comparison the indicated result in Figs. 4, 5 and 6, the opposite trend of receiver thermal efficiency and exergy efficiency is explained by the behavior of the exergy destruction due to heat transfer between the receiver and HTF, and heat losses due to heat transfer from receiver to the ambient. Results in Fig. 6 show that, the exergy efficiency of receiver is significantly affected by HTF type through the receiver. When ethylene glycol with alumina nanoparticle is selected as HTF through the receiver, the exergy efficiency is greater. Generally, in solar systems, the exergy efficiency is low, nevertheless, results in Fig. 6 show that, by selecting Nanofluids as HTF through the solar receivers, at least 20% enhancement in receiver exergy efficiency can be achieved. It should be noted that, although at specific value of HTF mass flow rate, the receiver thermal

efficiency is at its maximum value, but at the same value of HTF mass flow rate, the receiver exergy efficiency is at its minimum value.

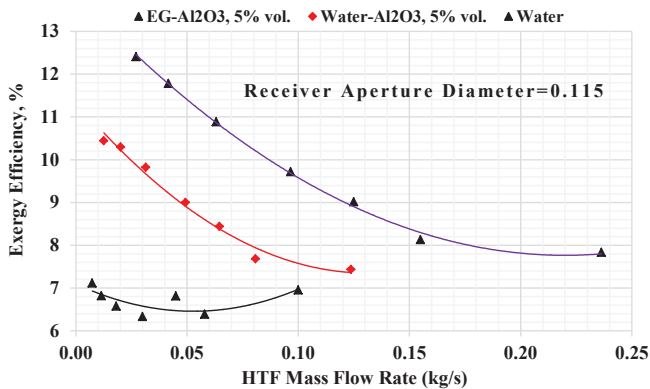


Fig. 6. Effect of HTF mass flow rate on receiver exergy efficiency.

5.4. Effect of nanoparticle volume fraction on receiver exergy efficiency

The effect of alumina volume fraction in the water as base fluid on receiver exergy efficiency is shown in Fig. 7. Results indicate that, when nanofluid with water as base fluid and 5% volume fraction alumina as nanoparticle is employed as HTF through the receiver compare to pure water, the greater exergy efficiency can be achieved. Also results reveal that, the effect of nanoparticle volume fraction on exergy efficiency for small HTF mass flow rates is greater than larger mass flow rates. By selecting only 5% volume of alumina nanoparticles in water, for small HTF mass flow rates, enhancement in exergy efficiency greater than 10% is attainable.

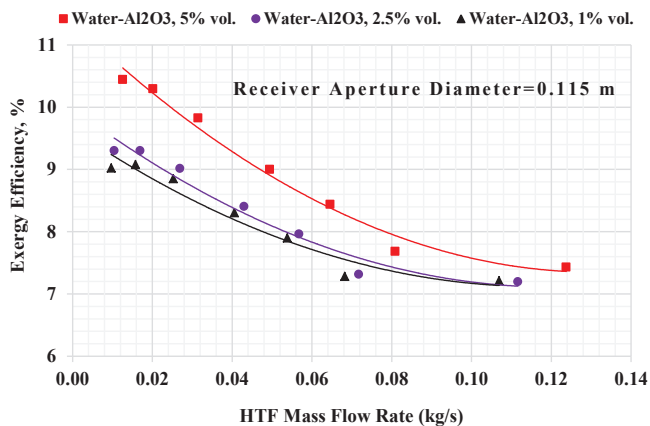


Fig. 7. The effect of nanoparticle volume fraction on receiver exergy efficiency.

6. Conclusions

As mentioned before, two approach are exist in thermal analysis of solar receivers. Isothermal receiver wall condition and constant isoflux receiver wall condition. In this study, the isothermal receiver wall condition is considered. For the system shown in Fig. 1, water is used as Heat Transfer Fluid through the receiver. Through experiments, HTF inlet and outlet temperatures, mass flow rate, solar irradiance and ambient air temperature and velocity are measured. Two unknown parameters in thermal analysis of such systems are exist: receiver average wall temperature and overall heat transfer coefficient. In experiment measuring the average receiver wall temperature is difficult and in some case is impossible. Therefore, by applying only the first thermodynamic law (energy analysis), thermal analysis cannot be carried out. Hence, the second thermodynamic law (exergy analysis) is essential. Based on these explanatory, an energy and exergy analysis are carried out on a cylindrical cavity receiver employed in a parabolic dish collector system. By simultaneous energy and exergy analysis of the system, the average receiver wall temperature and overall heat transfer coefficient are determined. By an energy balance on the receiver wall in contact with the HTF, a simplified Nusselt number as a function of Reynolds and Prandtl number is proposed. By using correlated Nusselt number, the effects of nanofluids on the system performance are investigated. The alumina nanoparticles in water and ethylene glycol as base fluid are studied. Based on the obtained results, the following important conclusions are proposed:

When nanofluids are employed as HTF through the receiver compare to pure water, the energy and exergy efficiency are greater. The minimum enhancement in receiver thermal efficiency is 25% and enhancement greater than 60% is attainable when nanofluids are employed as HTF through the receiver.

The effect of nanoparticle concentration in base fluid on energy and exergy efficiency of receiver is studied. The results indicate that, by increasing only 5% volume in nanoparticle concentration in water, the receiver thermal efficiency is increased greater than 20%.

The effect of nanoparticle volume fraction on exergy efficiency for small HTF mass flow rates is greater than larger mass flow rates. By selecting only 5% volume of alumina nanoparticle in water, for small HTF mass flow rates, enhancement in exergy efficiency greater than 10% is attainable.

Nomenclature

η_o	Optical efficiency
η_E	Exergy efficiency
A	Aperture area [m ²]
Q_l	The rate of total heat losses from the receiver to the surrounding [W]
I_b	Global solar irradiance per unit concentrator area [W/m ²]

HTF Heat Transfer Fluid

\dot{m}	HTF mass flow rate [kg/s]
c_p	HTF heat capacity [kJ/kg.K]
T	Temperature (K)
T_s	Black body temperature of the sun (K)
Nu_d	Nusselt number

Re_d Reynolds number

Pr Prandtl number

U_l Overall heat transfer coefficient [W/m².K]

h Convective heat transfer coefficient [W/m².K]

f_H Geometric factor

ΔP Pressure difference [Pa]

\dot{E} Exergy rate [W]

subscripts

r	Receiver
c	Concentrator
w	Wall
a	Ambient
out	Outlet
in	Inlet
$eff.$	Effective
0	Reference condition

$Th.$ Thermal

$Ex.$ Exergy

nf Nanofluid

bf Base fluid

np Nanoparticle

l Loss

Greek symbols

k Thermal conductivity [W/m.K]

ρ HTF density [kg/m³]

ε Emissivity

σ Stefan-Boltzmann constant, [W/(m².K⁴)]

μ HTF dynamic viscosity [kg/m.s]

ψ Maximum available work extracted from radiation reservoir

δ Half-angle of the cone subtending the concentrator [degree]

Ω Solid angle subtended by the mirrors [degree]

θ_0 Zenith angle [degree]

References

- [1] L. D. Jaffe, Dish concentrators for solar thermal energy, *J. Eng.* 7 (1983) 304-312.
- [2] T. P. Otanicar, J. S. Golden, Comparative environmental and economic analysis of conventional and nanofluid solar hot water technologies, *Environ. Sci. Technol.* 43 (2009) 6082-6087.
- [3] T. Yousefi, F. Veysi, E. Shojaeizadeh, S. Zinadini, An experimental investigation on the effect of Al₂O₃-H₂O nanofluid on the efficiency of flat-plate solar collectors, *Renew. Eng. J.* 39 (2012) 293-298.
- [4] L. Lu, Z. H. Liu, H. S. Xiao, Thermal performance of an open thermosyphon using nanofluids for high-temperature evacuated tubular solar collectors: Part 1: Indoor experiment, *Sol. Energy* 85 (2011) 379-387.

- [5] Y. Li, H. Q. Xie, W. Yu, J. Li, Investigation on heat transfer performances of nanofluids in solar collector, *Mater. Sci. Forum* 694 (2011) 33-36.
- [6] V. Khullar, H. Tyagi, P. E. Phelan, T. P. Otanicar, H. Singh, R. A. Taylor, Solar energy harvesting using nanofluids-based concentrating solar collector, *J. Nanotechnol. Eng. Med.* 3 (2013) 031003-1-031003-9.
- [7] R. A. Taylor, P. E. Phelan, T. P. Otanicar, C. A. Walker, M. Nguyen, S. Trimble, R. Prasher, Applicability of nanofluids in high flux solar collectors, *J. Renew. Sust. Energy* 3 (2011) 023104-1-023104-15.
- [8] A. Clausing, An analysis of convective losses from cavity solar central receivers, *Sol. Energy* 27 (1981) 295-300.
- [9] N. Kaushika, K. Reddy, Performance of a low cost solar paraboloidal dish steam generating system, *Energy Convers. Manage.* 41 (2000) 713-726.
- [10] N. Sendhil Kumar, K. Reddy, Comparison of receivers for solar dish collector system, *Energy Convers. Manage.* 49 (2008) 812-819.
- [11] N. Kaushika, Viability aspects of paraboloidal dish solar collector systems, *Renew. Eng. J.* 3 (1993) 787-793.
- [12] A. Kribus, P. Doron, R. Rubin, J. Karni, R. Reuven, S. Duchan, E. Taragan, A multistage solar receiver: The route to high temperature, *Sol. Energy* 67 (1999) 3-11.
- [13] M. Neber, H. Lee, Design of a high temperature cavity receiver for residential scale concentrated solar power, *Energy* 47 (2012) 481-487.
- [14] Y. Wang, X. Dong, J. Wei, H. Jin, Numerical simulation of the heat flux distribution in a solar cavity receiver, *Front. Energy Power Eng. Chin.* 4 (2010) 571-576.
- [15] J. Martinek, A.W. Weimer, Evaluation of finite volume solutions for radiative heat transfer in a closed cavity solar receiver for high temperature solar thermal processes, *Int. J. Heat. Mass. Tran.* 58 (2013) 585-596.
- [16] M. Prakash, S. Kedare, J. Nayak, Determination of stagnation and convective zones in a solar cavity receiver, *Int. J. Therm. Sci.* 49 (2010) 680-691.
- [17] V. Madadi, T. Tavakoli, A. Rahimi, First and second thermodynamic law analyses applied to a solar dish collector, *J. Non-Equilib. Thermodyn.* 39 (2014) 183-197.
- [18] Y. Wu, L. Wen, Solar receiver performance of point focusing collector system, *American Society of Mechanical Engineers (ASME)* 1 (1978).
- [19] R. Jilte, S. Kedare, J. Nayak, Natural convection and radiation heat loss from open cavities of different shapes and sizes used with dish concentrator, *Mech. Eng. Res.* 3 (2013) 26-43.
- [20] V. Badescu, Simple Upper Bound Efficiencies for Endoreversible Conversion of Thermal Radiation, *J. Non-Equilib. Thermodyn.* 24 (1999) 196-202.
- [21] V. Badescu, Lost available work and entropy generation: Heat versus radiation reservoirs, *J. Non-Equilib. Thermodyn.* 38 (2013) 313-333.
- [22] V. Badescu, How much work can be extracted from a radiation reservoir?, *Phys. A: Stat. Mech. Appl.* 410 (2014) 110-119.
- [23] R. Petela, Exergy of Heat Radiation, *J. Heat Transf.* 86 (1964) 187-192.
- [24] W. H. Press, Theoretical maximum for energy from direct and diffuse sunlight, *Nature* 264 (1976) 734-735.
- [25] A. Bejan, D. Kearney, F. Kreith, Second law analysis and synthesis of solar collector systems, *J. Sol. Energy Eng.* 103 (1981) 23-28.
- [26] A. Suzuki, General theory of exergy-balance analysis and application to solar collectors, *Energy* 13 (1988) 153-160.
- [27] M. J. Moran, H. N. Shapiro, D. D. Boettner, M. Bailey, *Fundamentals of engineering thermodynamics*, 7th ed., John Wiley and Sons, New York, 2011.
- [28] A. Suzuki, A fundamental equation for exergy balance on solar collectors, *J. Sol. Energy Eng.* 110 (1988) 102-106.
- [29] S. Kakaç, A. Pramuanjaroenkij, Review of convective heat transfer enhancement with nanofluids, *Int. J. Heat. Mass. Tran.* 52 (2009) 3187-3196.
- [30] S. Lee, S.-S. Choi, S. Li, and, J. Eastman, Measuring thermal conductivity of fluids containing oxide nanoparticles, *J. Heat Transf.* 121 (1999) 280-289.
- [31] R. K. Shah, A. L. London, *Laminar flow forced convection in ducts: a source book for compact heat exchanger analytical data*, Academic Press, New York, 1978.
- [32] M. A. Hachey, C. T. Nguyen, N. Galanis, C. V. Popa, Experimental investigation of Al_2O_3 nanofluids thermal properties and rheology – Effects of transient and steady-state heat exposure, *Int. J. Therm. Sci.* 76 (2014) 155-167.

